

Silencing of circ-PRKCH protects against lipopolysaccharide (LPS)-evoked chondrocyte damage and extracellular matrix loss by the miR-140-3p/ADAM10 axis

Jie Zhao¹, Tingting Li² and Wenming Luo¹

¹ Department of Traumatology and Orthopedics, Weifang People's Hospital, Weifang, Shandong, China

² Department of Ultrasound, Weifang Maternal and Child Health Hospital, Weifang, Shandong, China

Abstract. Circular RNAs (circRNAs) have been implicated in the pathology of osteoarthritis (OA). Nevertheless, the precise actions of circRNA protein kinase C eta (circ-PRKCH, hsa_circ_0032131) on OA pathogenesis are still undiscovered. Cell viability and apoptosis were determined using Cell Counting-8 Kit (CCK-8) assay and flow cytometry, respectively. The levels of circ-PRKCH, microRNA (miR)-140-3p and α -disintegrin and metalloproteinase domain 10 (ADAM10) mRNA were tested by quantitative real-time polymerase chain reaction (qRT-PCR) and Western blot. Targeted interplays among circ-PRKCH, miR-140-3p and ADAM10 were verified by dual-luciferase reporter assay. circ-PRKCH was up-regulated in OA tissues and lipopolysaccharide (LPS)-evoked C-28/I2 cells. circ-PRKCH knockdown alleviated LPS-evoked cell injury and extracellular matrix (ECM) loss in C-28/I2 cells. Mechanistically, circ-PRKCH acted as a miR-140-3p sponge. Moreover, the silencing of circ-PRKCH exerted a protective role in LPS-evoked C-28/I2 cells by up-regulating miR-140-3p. ADAM10 was a direct target of miR-140-3p, and miR-140-3p overexpression mitigated LPS-evoked C-28/I2 cell injury and ECM loss by down-regulating ADAM10. Furthermore, circ-PRKCH mediated ADAM10 expression *via* sponging miR-140-3p in C-28/I2 cells. Our present study suggested that circ-PRKCH silencing alleviated LPS-evoked chondrocyte injury and ECM loss partially through the miR-140-3p/ADAM10 axis.

Key words: Osteoarthritis — circ-PRKCH — miR-140-3p — ADAM10

Introduction

Osteoarthritis (OA), the most prevalent joint disorder, affects the health in the elderly population worldwide (Martel-Pelletier et al. 2016). OA is mainly caused by extravagant chondrocyte death and extracellular matrix (ECM) loss in articular cartilage (Charlier et al. 2019). Despite developed primary care and surgery, effective treatments remain insufficient (Oo et al. 2018). A better understanding for the mechanisms of the occurrence and progression of OA will help to make a breakthrough in OA innovative therapies.

Circular RNAs (circRNAs) are a novel class of noncoding RNAs with backsplice junction *via* covalently linked 3'-5' ends, which serve as key players in normal development and

disease (Patop et al. 2019). Recent studies also highlight that some circRNAs directly interact with microRNAs (miRNAs) through sequestration (Verduci et al. 2019), and numerous circRNAs implicate in the occurrence and progression of OA (Zhou et al. 2018; Xiao et al. 2019). Zhou et al. (2019b) uncovered that circRNA.33186 was overexpressed in the OA animal and cell model, and the depletion of circRNA.33186 restrained OA progression *via* mediating matrix metalloproteinase-13 (MMP-13) expression by sponging miR-127-5p. Liu et al. (2016) underscored that circRNA related to the chondrocyte ECM (circRNA-CER) accelerated chondrocyte inflammation, and its down-regulation promoted ECM formation through targeting the miR-136/MMP13 axis. Shen and colleagues demonstrated that circRNA serpin family E member 2 (circ-SERPINE2) level was reduced in the OA cartilage tissues, and the elevated circSERPINE2 expression weakened chondrocyte apoptosis and enhanced ECM formation by the regulation of the miR-1271-5p/E26 transformation-specific-related gene (ERG) axis (Shen et al. 2019). As for circRNA protein

Correspondence to: Wenming Luo, Department of Traumatology and Orthopedics, Weifang People's Hospital, 151 Guangwen Street, Kuiwen District, Weifang, Shandong, 261041, China
E-mail: vyisrf@163.com

kinase C eta (circ-PRKCH, hsa_circ_0032131), derived from PRKCH gene which is associated with OA pathogenesis (Wang et al. 2015), it was discovered to be up-regulated in the peripheral blood of patients with OA (Wang et al. 2019). Nevertheless, the function and mechanism of circ-PRKCH on OA pathogenesis are still undiscovered.

miRNAs have been widely recognized to be relevant to OA pathology (Malemud 2018). miR-140-3p was reported to be the most significantly up-regulated miRNA in healthy cartilage (Karlsen et al. 2014). Earlier researches had uncovered that miR-140-3p expression was strongly decreased in OA and was negatively associated with OA severity (Ntoumou et al. 2017; Yin et al. 2017). Moreover, the up-regulation of miR-140-3p played a protective role in OA aggravation (Al-Modawi et al. 2019). When we used several computational methods to help identify the mechanism of circ-PRKCH in OA pathogenesis, we found two complementary sites among circ-PRKCH, miR-140-3p and a-disintegrin and metalloproteinase domain 10 (ADAM10), which prompted us to inspect the miR-140-3p/ADAM10 axis as a molecular mediator of circ-PRKCH in OA progression.

In the current project, we initially constructed an *in vitro* model of OA by lipopolysaccharide (LPS)-evoked chondrocytes. Subsequently, we investigated the function and mechanism of circ-PRKCH on LPS-evoked chondrocyte injury and ECM loss.

Materials and Methods

Tissue samples

All procedures were approved by the Ethics Committee of Weifang People's Hospital. 30 OA cartilage samples were collected from the tissues excised during knee replacement surgery from OA patients (range = 46–72 years, mean age = 62.5 years) at Weifang People's Hospital. Thirty healthy knee cartilage samples were taken from volunteers (range = 40–76 years, mean age = 59.7 years, no known history of OA or rheumatoid arthritis) who underwent an amputation due to an accidental injury. The fresh tissue samples were stored at -80°C in RNAlater stabilization solution (Invitrogen, Merelbeke, Belgium). Written informed consent was provided by all subjects.

Cell culture and treatment

C-28/I2 (Bnbio, Beijing, China), an immortalized chondrocyte cell line, was used in the current project. Cells were cultured at 37°C and 5% CO_2 using Dulbecco's Modified Eagle's Medium/Ham's F-12 medium (1:1, DMEM/F-12, Invitrogen) and 10% fetal bovine serum (FBS, Mediatech, HongKong, China). To construct an *in vitro* model of OA,

C-28/I2 cells in 24-well plates were allowed to reach about 70% confluence, followed by the stimulation with LPS (Sigma-Aldrich, Toyko, Japan) at final concentrations of 1, 5 and 10 $\mu\text{g}/\text{ml}$ for 24 h.

Cell transfection

siRNA against circ-PRKCH (si-circ-PRKCH, 5'-GGGATCCTAAAATCTAGATCT-3') and nontarget siRNA (si-NC, 5'-UUCUCCGAACGUGUCACGUTT-3'), the commercial miR-140-3p mimic (5'-GGCACCAAGAUGGGACACCAU-3') and mimic negative control (miR-NC mimic, 5'-UUCUCCGAACGUGUCACGUTT-3'), the synthetic inhibitor of miR-140-3p (anti-miR-140-3p, 5'-AUGGUGUCCCAUCUUGGUGCC-3') and corresponding negative control (anti-miR-NC, 5'-CAGUACUUUUGUGUAGUACAA-3'), pcDNA-based circ-PRKCH and ADAM10 overexpression plasmids (circ-PRKCH and ADAM10) and nontarget plasmid (pcDNA) were procured from GenePharma (Shanghai, China). The available transfection reagent Lipofectamine 3000 (Invitrogen) was utilized for various transfections of the indicated oligonucleotide (20 nM) and/or plasmid (100 ng) as recommended by the manufacturers. Detection of transfection efficiency was conducted 24 h post-transfection by quantitative real-time polymerase chain reaction (qRT-PCR).

Measurement of cell viability and apoptosis

C-28/I2 cells were subjected to LPS treatment as described above or various transfections followed by 5 $\mu\text{g}/\text{ml}$ of LPS challenge for 24 h. Cell viability was tested using a colorimetric Cell Counting-8 Kit (CCK-8, Yesen, Shanghai, China) based on the recommendation of producers. The number of viable cells was proportional to the 450 nM absorbance detecting by a microplate reader (Viktor X3, Perkin Elmer, Turku, Finland). Cell apoptosis assessment was carried out by flow cytometry using the Invitrogen Annexin V-FITC/propidium iodide (PI) Kit as recommended by the manufacturers. A total of $\sim 10,000$ events *per* sample was used for the analysis of the apoptotic rate by a flow cytometer (BD Biosciences, Erembodegem, Belgium).

Enzyme-linked immunosorbent assay (ELISA)

The levels of interleukin-8 (IL-8), tumor necrosis factor- α (TNF- α) and IL-1 β in the cell supernatant were determined using ELISA assay kits (Invitrogen) based on the manufacturer's suggestion.

Western blot

The cartilage samples and C-28/I2 cells were solubilized in RIPA buffer (Beyotime, Shanghai, China) and Western blot

analyses were implemented after SDS polyacrylamide gel electrophoresis as previously reported (Xie et al. 2020). The primary antibodies used for immunoblotting were anti-type II collagen (anti-Col2A1, sc-52658; dilution 1:500), anti-Agrecan (sc-33695; dilution 1:1000), anti-B cell lymphoma 2 (anti-Bcl-2, sc-7382; dilution 1:500), anti-ki-67 (sc-23900; dilution 1:1000), anti-ADAM10 (sc-48400; dilution 1:500) and a loading buffer anti-glyceraldehyde-3-phosphate dehydrogenase (anti-GAPDH, sc-47724; dilution 1:1000); all from Santa Cruz Biotechnology, Santa Cruz, CA, USA. Horseradish peroxidase conjugated anti-IgG (sc-2748; dilution 1:1000; Santa Cruz Biotechnology) was used as secondary antibody. The signals were developed using the Chemiluminescent Kit (Beyotime) as recommended by manufacturers.

qRT-PCR

Total RNA from cartilage samples and C-28/I2 cells was extracted by homogenization in TRIzol reagent (Invitrogen) and was quantified by a Bioanalyzer (Bio-Rad, Glattbrugg, Switzerland) at 260 nm. For circ-PRKCH and ADAM10 mRNA quantification, cDNA was generated using the Bio-Rad iScript Kit and qRT-PCR was performed using Bio-Rad SYBR Green Supermix as recommended by the manufacturers. The TaqMan MicroRNA Reverse Transcription Kit and TaqMan universal master mix (Applied Biosystems, Courtaboeuf, France) were used for miR-140-3p quantification. Analysis was conducted using the $2^{-\Delta\Delta Ct}$ approach (Rivetti di Val Cervo et al. 2012) with β -actin or U6 as an internal reference gene. The PCR primers for circ-PRKCH, miR-140-3p and ADAM10 mRNA were listed in Table 1.

Bioinformatics and dual-luciferase reporter assay

The potentially interacted miRNAs of circ-PRKCH were predicted using the online CircInteractome database (<https://circinteractome.nia.nih.gov/index.html>). The puta-

tive targets of miR-140-3p were searched by the starbase v.3 software (<http://starbase.sysu.edu.cn/>). The wild-type circ-PRKCH reporter construct (WT-circ-PRKCH) harboring the target sequence of miR-140-3p and the mutant-type circ-PRKCH construct (MUT-circ-PRKCH, from CUGUGGU to GACACCA), and ADAM10 3'UTR reporter construct (WT-ADAM10 3'UTR) and the mutation of the target region (MUT-ADAM10 3'UTR, from CCUGUGGU to GGACACCA) were produced by Uptbio (Changsha, China). The four reporter constructs (100 ng) were individually transiently introduced into C-28/I2 cells, together with 20 nM of miR-140-3p mimic or miR-NC mimic. The cells were lysed 24 h post-transfection and then analyzed for luciferase activity using the dual luciferase assay (Promega, Southampton, UK) based on the manufacturer's directions.

Statistical analysis

Each treatment was carried out at least three biological and technical replications, and data were reported as mean \pm standard error of the mean. The differences between the different groups were compared using a Student's *t*-test or one-way analysis of variance (ANOVA) followed by the Tukey's multiple comparison test. The Spearman test was used for the determination of correlation among circ-PRKCH, miR-140-3p and ADAM10 in OA samples. Statistical significance was defined at $p < 0.05$.

Results

LPS induced cell injury and ECM loss of C-28/I2 cells

To construct an *in vitro* model of OA, C-28/I2 cells were treated with various concentrations of LPS. CCK-8 and flow cytometry assays revealed that in contrast to the negative control, cell viability was significantly reduced (Fig. 1A) and cell apoptosis was remarkably promoted (Fig. 1B) by the

Table 1. Primers for PCR

Primers for PCR (5'-3')		
circ_PRKCH	Forward	GGCAGAGAACGAAGATGACC
	Reverse	CATTCCGAAGTCTGCCAGTT
miR-140-3p	Forward	ACACTCCAGCTGGGAGGCGGGGCGCCGCGGGA
	Reverse	CTCAACTGGTGTCTGTGGA
ADAM10	Forward	ATATTACGGAACACGAGAAGCTG
	Reverse	TCAATCGCTTTAACATGACTGG
β -actin	Forward	GCACCACACCTTCTACAATG
	Reverse	TGCTTGCTGATCCACATCTG
U6	Forward	CTCGCTTCGGCAGCACA
	Reverse	AACGCTTCACGAATTTGCGT

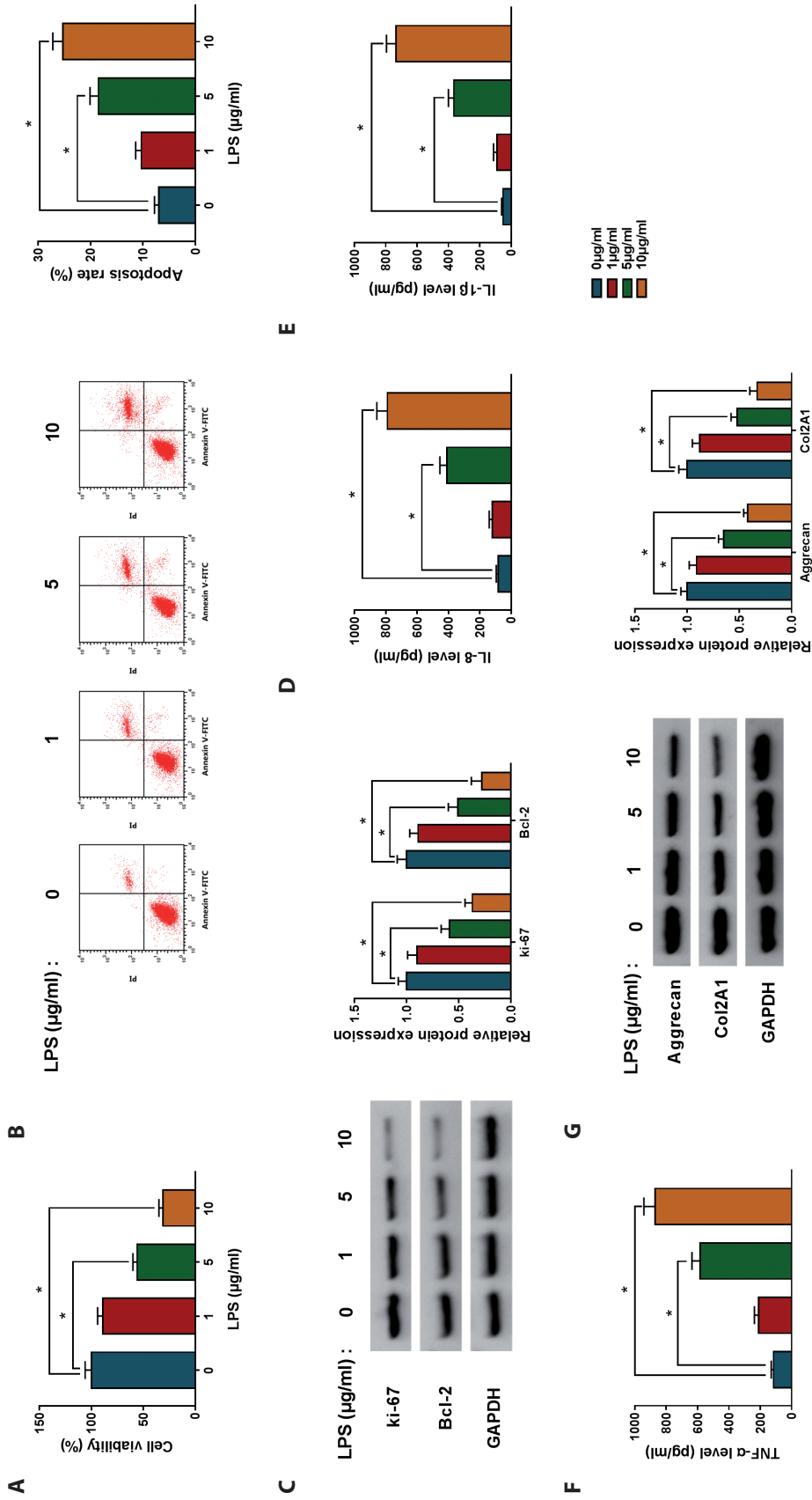


Figure 1. LPS induced C-28/I2 cell damage and ECM loss. C-28/I2 cells were treated with various concentrations (0, 1, 5 and 10 µg/ml) of LPS for 24 h. **A.** CCK-8 assay for cell viability. **B.** Flow cytometry for cell apoptosis. **C.** Western blot for Bcl-2 and ki-67 levels in treated cells. ELISA assay for IL-8 (**D**), IL-1β (**E**) and TNF-α (**F**) levels in LPS-stimulated cells. **G.** Western blot for Aggrecan and Col2A1 expression in treated cells. * $p < 0.05$ by ANOVA followed by Tukey-Kramer *post hoc* test. LPS, lipopolysaccharide; ECM, extracellular matrix; Bcl-2, B-cell lymphoma 2; Col2A1, type II collagen; GAPDH, glyceraldehyde-3-phosphate dehydrogenase; IL, interleukin; TNF-α, tumor necrosis factor-α.

stimulation with 5 and 10 $\mu\text{g/ml}$ of LPS. Moreover, Western blot data showed that LPS led to a decrease in the levels of proliferating marker ki-67 and anti-apoptotic protein Bcl-2 in C-28/I2 cells (Fig. 1C), supporting LPS-mediated viability suppression and apoptosis promotion. ELISA analyses showed that LPS treatment led to a striking increase in the production of pro-inflammatory cytokines IL-8, IL-1 β and TNF- α in a dose-dependent manner in C-28/I2 cells (Fig. 1D–F), indicating the enhanced impact of LPS on cell inflammation. These data together indicated that LPS induced chondrocyte damage by inhibiting cell viability and promoting cell apoptosis and inflammation. Furthermore, LPS (5 and 10 $\mu\text{g/ml}$) stimulation resulted in decreased levels of Aggrecan and Col2A1, the two main components of cartilage ECM (Fig. 1G).

circ-PRKCH was up-regulated and miR-140-3p was down-regulated in OA tissues and LPS-evoked C-28/I2 cells

To preliminary observation the involvement of circ-PRKCH and miR-140-3p in OA, we determined their expression levels in OA tissues and LPS-evoked C-28/I2 cells. As shown

by qRT-PCR, in comparison to the corresponding control group, circ-PRKCH level was prominently elevated in OA tissues (Fig. 2A), and LPS stimulation dose-dependently increased the expression of circ-PRKCH in C-28/I2 cells (Fig. 2B). Conversely, OA patients had a lower miR-140-3p expression than that of control (Fig. 2C), and miR-140-3p level was significantly reduced by LPS treatment in C-28/I2 cells (Fig. 2D). Interestingly, an inverse correlation between circ-PRKCH level and miR-140-3p expression was discovered in OA tissues (Fig. 2E).

Silencing of circ-PRKCH mitigated LPS-evoked cell injury and ECM loss in C-28/I2 cells

To explore whether circ-PRKCH could affect OA progression, we then performed loss-of-function analyses using si-circ-PRKCH. Transient introduction of si-circ-PRKCH, but not the si-NC control, dramatically decreased the level of circ-PRKCH, which was elevated by LPS in C-28/I2 cells (Fig. 3A). Function experiments results revealed that in contrast to the negative control, LPS-evoked anti-viability and pro-apoptosis effects were notably abolished by circ-PRKCH

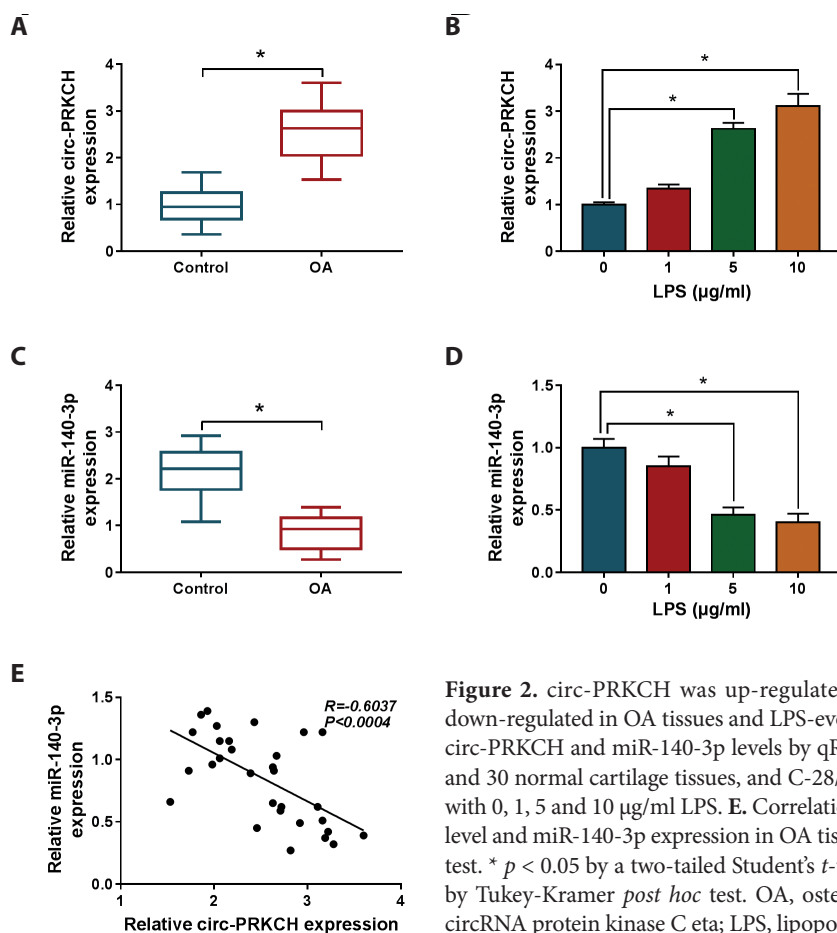


Figure 2. circ-PRKCH was up-regulated and miR-140-3p was down-regulated in OA tissues and LPS-evoked C-28/I2 cells. **A–D.** circ-PRKCH and miR-140-3p levels by qRT-PCR in 30 OA tissues and 30 normal cartilage tissues, and C-28/I2 cells after stimulation with 0, 1, 5 and 10 $\mu\text{g/ml}$ LPS. **E.** Correlation between circ-PRKCH level and miR-140-3p expression in OA tissues using the Spearman test. * $p < 0.05$ by a two-tailed Student's t -test or ANOVA followed by Tukey-Kramer *post hoc* test. OA, osteoarthritis; circ-PRKCH, circRNA protein kinase C eta; LPS, lipopolysaccharide.

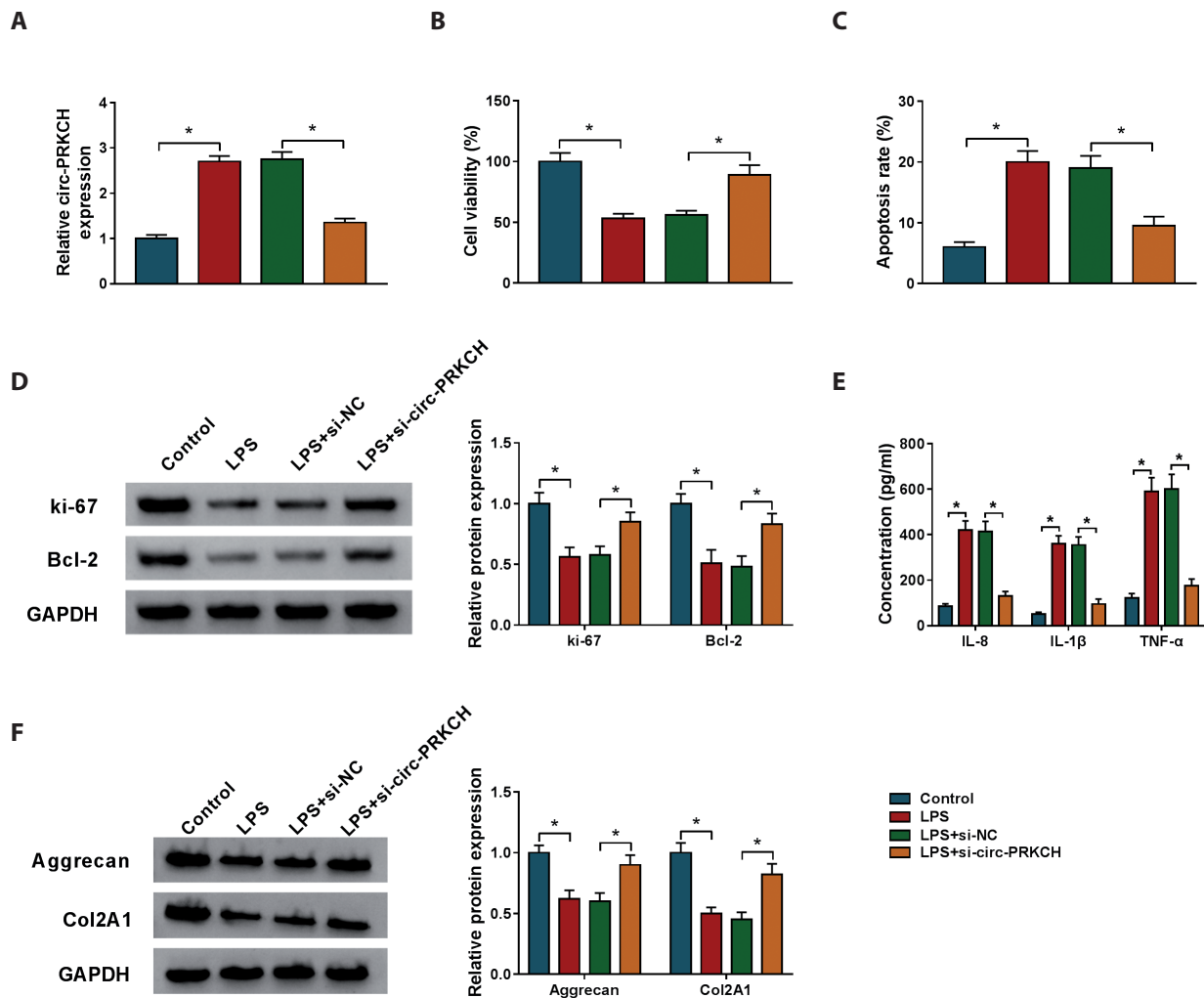


Figure 3. Silencing of circ-PRKCH alleviated LPS-evoked C-28/I2 cell damage and ECM loss. C-28/I2 cells were transfected with si-circ-PRKCH or si-NC, and then were treated with 5 μ g/ml LPS for 24 h. **A.** circ-PRKCH expression by qRT-PCR in treated cells. **B.** Cell viability by CCK-8 assay. **C.** Cell apoptosis by flow cytometry. **D.** Western blot for Bcl-2 and ki-67 levels in treated cells. **E.** The levels of IL-8, IL-1 β and TNF- α by ELISA assay in treated cells. **F.** Aggrecan and Col2A1 levels by Western blot in treated cells. * $p < 0.05$ by ANOVA followed by Tukey-Kramer *post hoc* test. si-NC, negative control siRNA; si-circ-PRKCH, siRNA targeting circ-PRKCH. For more abbreviations, see Fig. 1 and 2.

knockdown (Fig. 3B–D). Moreover, the enhanced impact of LPS on IL-8, IL-1 β and TNF- α production was significantly reversed by the silencing of circ-PRKCH in C-28/I2 cells (Fig. 3E). Additionally, LPS-mediated Aggrecan and Col2A1 diminishment in C-28/I2 cells was prominently abrogated by circ-PRKCH silencing (Fig. 3F).

circ-PRKCH acted as a miR-140-3p sponge and circ-PRKCH silencing exerted a protective role in LPS-evoked C-28/I2 cells by miR-140-3p

We next determined the mechanism by which circ-PRKCH regulated LPS-evoked cell injury and ECM loss. Bioinformatic

analysis for the interacted miRNAs of circ-PRKCH showed that it harbored seven nucleotides of sequence complementarity to the miR-140-3p seed region (Fig. 4A). Transient transfection of miR-140-3p mimic, but not the miR-NC control, remarkably reduced the activity of luciferase reporter gene fused on the wild-type circ-PRKCH reporter (WT-circ-PRKCH, Fig. 4B). However, little change was observed in luciferase activity of mutant-type circ-PRKCH construct (MUT-circ-PRKCH) in the presence of miR-140-3p mimic (Fig. 4B). qRT-PCR data showed that circ-PRKCH expression was notably increased by the corresponding overexpression plasmid (Fig. 4C). Moreover, in comparison to their counterparts, miR-140-

3p expression was significantly increased by circ-PRKCH silencing and was highly decreased when circ-PRKCH up-regulation in C-28/I2 cells (Fig. 4D). These data together strongly pointed the role of circ-PRKCH as a sponge of miR-140-3p.

To assess whether miR-140-3p was involved in circ-PRKCH-mediated regulation on LPS-evoked cell injury and ECM loss, C-28/I2 cells were cotransfected with si-circ-PRKCH and anti-miR-140-3p before LPS stimulation. The data of qRT-PCR revealed a striking down-regulation of miR-140-3p in the anti-miR-140-3p-transfecting cells (Fig. 4E). Further function analyses showed that in comparison to the negative control, si-circ-PRKCH-mediated pro-viability, anti-apoptosis and anti-inflammation effects were dramatically reversed by miR-140-3p knockdown in LPS-evoked C-28/I2 cells (Fig. 4F–I). Furthermore, the increased impact of circ-PRKCH silencing on Aggrecan and Col2A1 levels was prominently abolished by the depletion of miR-140-3p in C-28/I2 cells under LPS (Fig. 4J).

ADAM10 was directly targeted and repressed by miR-140-3p

miRNAs exert biological function through silencing gene expression. To identify the targets of miR-140-3p, the star-Base v.3 online software was used, and the data revealed a putative target sequence for miR-140-3p in the 3'UTR of ADAM10 (Fig. 5A). Transfection of ADAM10 3'UTR reporter construct (WT-ADAM10 3'UTR) in the presence of miR-140-3p mimic led to a striking reduction in luciferase activity, and this effect was completely abolished by the mutation of the target region (MUT-ADAM10 3'UTR, Fig. 5B). The data of qRT-PCR and Western blot assays showed that in comparison to their counterparts, ADAM10 was highly expressed at both mRNA and protein levels in OA tissues and LPS-evoked C-28/I2 cells (Fig. 5C–F). Excitingly, ADAM10 mRNA expression was inversely correlated with miR-140-3p level in OA tissues (Fig. 5G). qRT-PCR data also revealed that miR-140-3p was up-regulated in miR-140-3p mimic-transfecting cells (Fig. 5H). Additionally, ADAM10 level was significantly reduced by miR-140-3p overexpression and elevated following miR-140-3p depletion in C-28/I2 cells (Fig. 5I).

Overexpression of miR-140-3p alleviated LPS-evoked C-28/I2 cell injury and ECM loss by down-regulating ADAM10

Transfection of ADAM10 overexpression plasmid led to a prominent elevation in ADAM10 expression at both mRNA and protein levels in C-28/I2 cells (Fig. 6A,B). Subsequent experiments data revealed that in contrast to the miR-NC group, miR-140-3p overexpression triggered a significant enhancement in cell viability and a distinct repression in cell apoptosis (Fig. 6C–E), as well as a striking reduction

in the production of IL-8, IL-1 β and TNF- α (Fig. 6F) in LPS-treated C-28/I2 cells. Moreover, the elevated miR-140-3p expression resulted in increased Aggrecan and Col2A1 levels in LPS-induced C-28/I2 cells (Fig. 6G). Nevertheless, these effects of miR-140-3p overexpression were remarkably abrogated by ADAM10 up-regulation in LPS-induced C-28/I2 cells (Fig. 6C–G).

circ-PRKCH regulated ADAM10 expression through sponging miR-140-3p

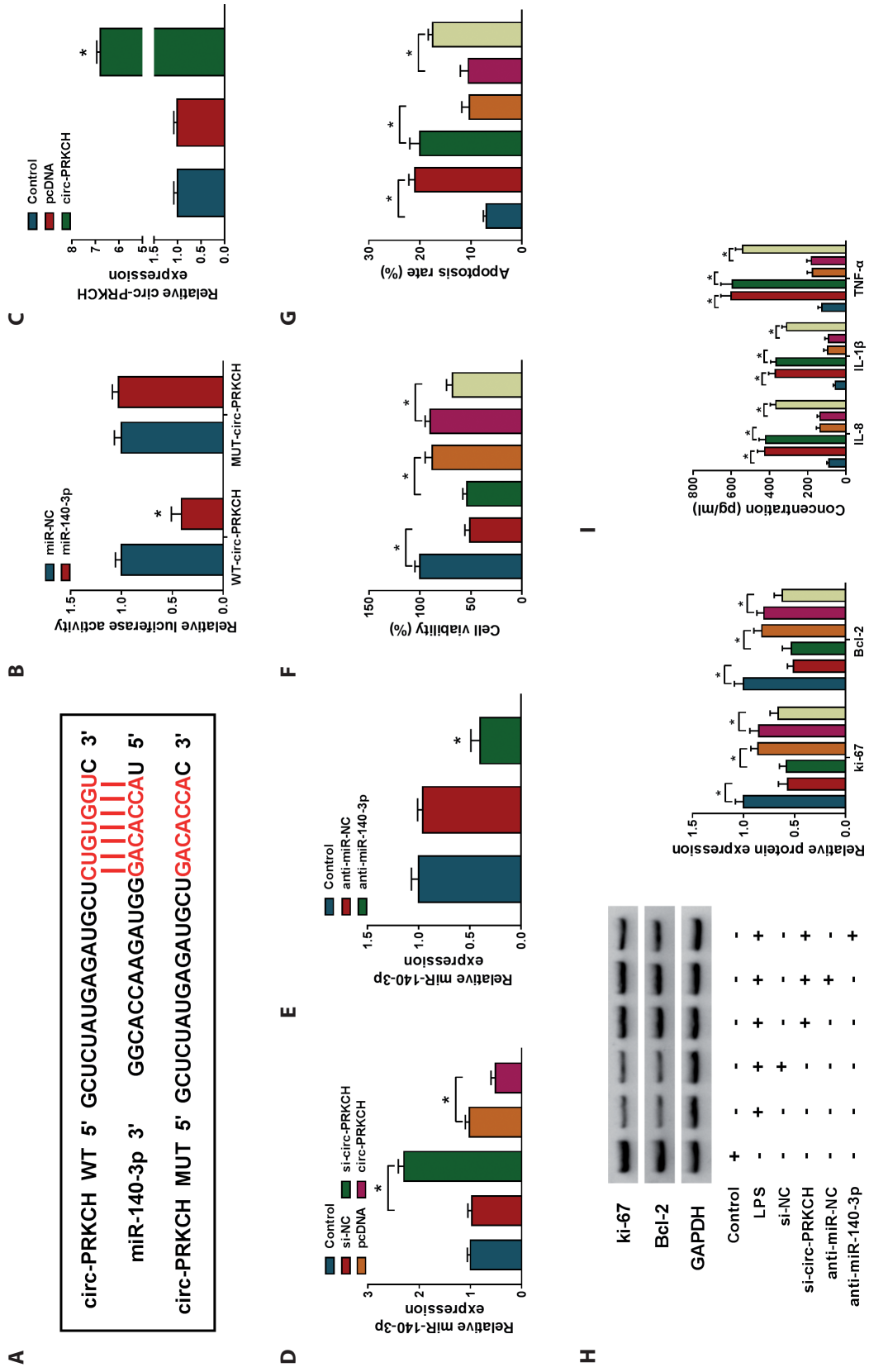
Lastly, we explored whether circ-PRKCH mediated ADAM10 expression in C-28/I2 cells. Interestingly, in comparison to the corresponding control, ADAM10 protein expression was prominently down-regulated by circ-PRKCH silencing in C-28/I2 cells. However, this effect was dramatically abolished by the transfection of anti-miR-140-3p (Fig. 7).

Discussion

OA is a debilitating joint disease with a high morbidity in the elderly population; however, little effective strategies are available to prevent OA development because of the inadequate understanding of OA pathology (Ebell 2018). Recently, circRNAs have been underscored as essential players in the pathogenesis of a wide variety of human diseases (Han et al. 2018). Nevertheless, it is still largely undefined about their roles in the occurrence and progression of OA. In this investigation, we explored whether circ-PRKCH affected LPS-evoked chondrocyte injury and ECM loss and whether the miR-140-3p/ADAM10 axis was involved in the regulatory networks of circ-PRKCH in OA.

LPS could promote chondrocyte inflammation and degeneration and trigger ECM expression, thereby contributing to OA progression (Wang 2018; Qing et al. 2019). Here, firstly, we successfully constructed an *in vitro* model of OA by LPS. Interestingly, we discovered that circ-PRKCH was highly expressed in OA cartilage samples and LPS elevated the expression of circ-PRKCH in C-28/I2 chondrocyte cells, supporting the finding by Wang et al. (2019). For the first time, we disclosed that the silencing of circ-PRKCH retarded LPS-evoked chondrocyte injury and ECM loss, as evidenced by the promotion in cell viability and the suppression in cell apoptosis and inflammation, as well as the increase in Aggrecan and Col2A1 levels.

circRNAs exert critical function in human diseases *via* mediating gene expression through acting as effective miRNA sponges (Panda 2018). We then predicted the interacted miRNAs of circ-PRKCH using the CircInteractome database (Dudekula et al. 2016), and we verified that circ-PRKCH functioned as a sponge of miR-140-3p. Increasing evidence has shown that miR-140-3p plays a key role in a series of



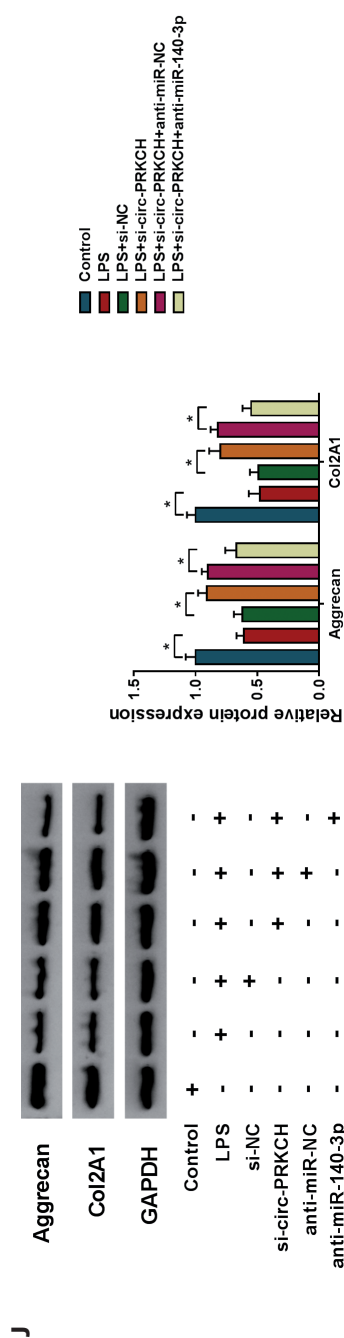


Figure 4. circ-PRKCH acted as a miR-140-3p sponge and circ-PRKCH silencing relieved LPS-evoked cell damage and ECM loss by miR-140-3p. **A.** Schematic of the complementary sequence of miR-140-3p within circ-PRKCH and mutated miR-140-3p seed region. **B.** Relative luciferase activity in C-28/I2 cells cotransfected with WT-circ-PRKCH or MUT-circ-PRKCH and miR-140-3p mimic or miR-NC mimic. **C.** qRT-PCR for circ-PRKCH expression in C-28/I2 cells transfected with or without pcDNA or circ-PRKCH overexpression plasmid. **D, E.** qRT-PCR for miR-140-3p level in C-28/I2 cells transfected with or without si-NC, si-circ-PRKCH, pcDNA, circ-PRKCH overexpression plasmid, anti-miR-NC or anti-miR-140-3p. C-28/I2 cells were transfected with si-NC, si-circ-PRKCH, si-circ-PRKCH+anti-miR-NC or si-circ-PRKCH+anti-miR-140-3p before 5 μ g/ml LPS stimulation, followed by the determination of cell viability by CCK-8 assay (**F**), cell apoptosis by flow cytometry (**G**), Bcl-2 and ki-67 levels by Western blot (**H**), IL-8, IL-1 β and TNF- α levels by ELISA assay (**I**), and Aggrecan and Col2A1 levels by Western blot (**J**). * $p < 0.05$ by a two-tailed Student's *t*-test or ANOVA followed by Tukey-Kramer *post hoc* test. pcDNA, negative control plasmid; anti-miR-NC, negative control miRNA inhibitor; anti-miR-140-3p, miR-140-3p inhibitor; WT-circ-PRKCH, circ-PRKCH wild-type reporter construct; MUT-circ-PRKCH, circ-PRKCH mutant-type reporter construct. For more abbreviations, see Fig. 1 and 3.

human diseases. For instance, Zhu et al. (2018) reported that miR-140-3p level was decreased in peripheral artery disease, and it regulated the In-Stent Restenosis by targeting B cell lymphoma-2. Liu et al. (2019) underscored that the elevated miR-140-3p expression accelerated fracture healing by activating the Wnt pathway. Moreover, miR-140-3p was identified to hinder the progression of multiple tumors, such as breast cancer and colorectal cancer (Jiang et al. 2019; Zhou et al. 2019a). In this work, we observed a prominent down-regulation of miR-140-3p in OA samples and LPS-evoked chondrocytes, in agreement with former studies (Ntounou et al. 2017; Yin et al. 2017). We also validated that miR-140-3p overexpression exerted a protective effect in LPS-evoked chondrocyte injury and ECM loss, consistent with recent work (Al-Modawi et al. 2019). More interestingly, we were first to highlight that circ-PRKCH silencing alleviated LPS-evoked chondrocyte injury and ECM loss by up-regulating miR-140-3p.

We subsequently testified that ADAM10 in C-28/I2 cells was directly targeted and repressed by miR-140-3p. Among these predicted targets of miR-140-3p by the starBase v.3 software, ADAM10 caught our attention owing to its essential effect in skeletal growth and bone remodeling in humans and mice (Dallas et al. 1999; Mizuno et al. 2020). ADAM10 expression was reported to be increased in OA cartilage, and overexpressed ADAM10 led to cartilage injury (Chubinskaya et al. 2001; Yang et al. 2017). Moreover, the elevated ADAM10 expression could promote CD44 cleavage, giving rise to ECM loss in human chondrocytes (Kobayakawa et al. 2016). Additionally, ADAM10 was involved in the regulation of miR-20a on human arthritis progression and inflammation (Xie et al. 2020). Herein, we first uncovered that miR-140-3p overexpression alleviated LPS-evoked chondrocyte injury and ECM loss by down-regulating ADAM10. Zafar and colleagues underscored that miR-140-3p was correlated with OA pathogenesis *via* targeting ADAMTS5 (Rasheed et al. 2018). Furthermore, for the first time, we highlighted that circ-PRKCH protected against ADAM10 repression by acting as a miR-140-3p sponge. Previous evidence had shown that ADAM10 regulated the activation of Notch and NF- κ B signaling pathways (Toonen et al. 2016; Alabi et al. 2018), which are implicated in OA progression (Saito et al. 2017). Therefore, more investigations about the relationship between the circ-PRKCH/miR-140-3p/ADAM10 axis and the two pathways on OA pathogenesis will be explored in further work. Besides, the current work was limited to *in vitro* investigations, and more *in vivo* studies about the new mechanism using the OA animal model is expected to be carried out in further work.

In conclusion, the present work demonstrated that circ-PRKCH silencing alleviated LPS-evoked chondrocyte injury and ECM loss at least partly *via* regulating ADAM10 expres-

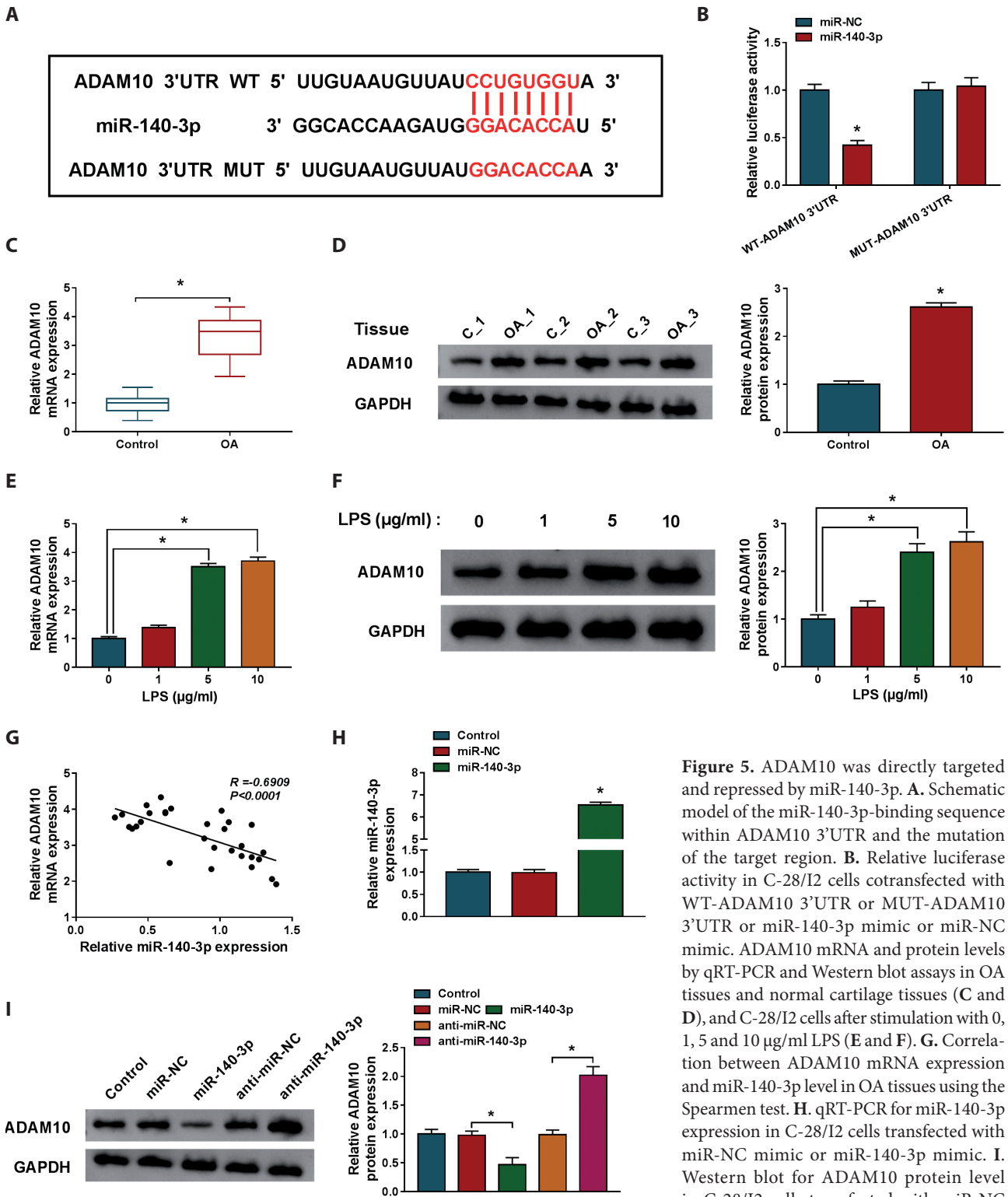


Figure 5. ADAM10 was directly targeted and repressed by miR-140-3p. **A.** Schematic model of the miR-140-3p-binding sequence within ADAM10 3'UTR and the mutation of the target region. **B.** Relative luciferase activity in C-28/I2 cells cotransfected with WT-ADAM10 3'UTR or MUT-ADAM10 3'UTR or miR-140-3p mimic or miR-NC mimic. ADAM10 mRNA and protein levels by qRT-PCR and Western blot assays in OA tissues and normal cartilage tissues (C and D), and C-28/I2 cells after stimulation with 0, 1, 5 and 10 µg/ml LPS (E and F). **G.** Correlation between ADAM10 mRNA expression and miR-140-3p level in OA tissues using the Spearman test. **H.** qRT-PCR for miR-140-3p expression in C-28/I2 cells transfected with miR-NC mimic or miR-140-3p mimic. **I.** Western blot for ADAM10 protein level in C-28/I2 cells transfected with miR-NC mimic, miR-140-3p mimic, anti-miR-NC

or anti-miR-140-3p. * $p < 0.05$ by a two-tailed Student's *t*-test or ANOVA followed by Tukey-Kramer *post hoc* test. OA, osteoarthritis; anti-miR-NC, negative control miRNA inhibitor; anti-miR-140-3p, miR-140-3p inhibitor; ADAM10, a-disintegrin and metallopeptidase domain 10; miR-NC, negative control mimic; miR-140-3p, miR-140-3p mimic; WT-ADAM10 3'UTR, ADAM10 3'UTR wild-type reporter construct; MUT-ADAM10 3'UTR, ADAM10 3'UTR mutant-type reporter construct. For more abbreviations, see Fig. 1.

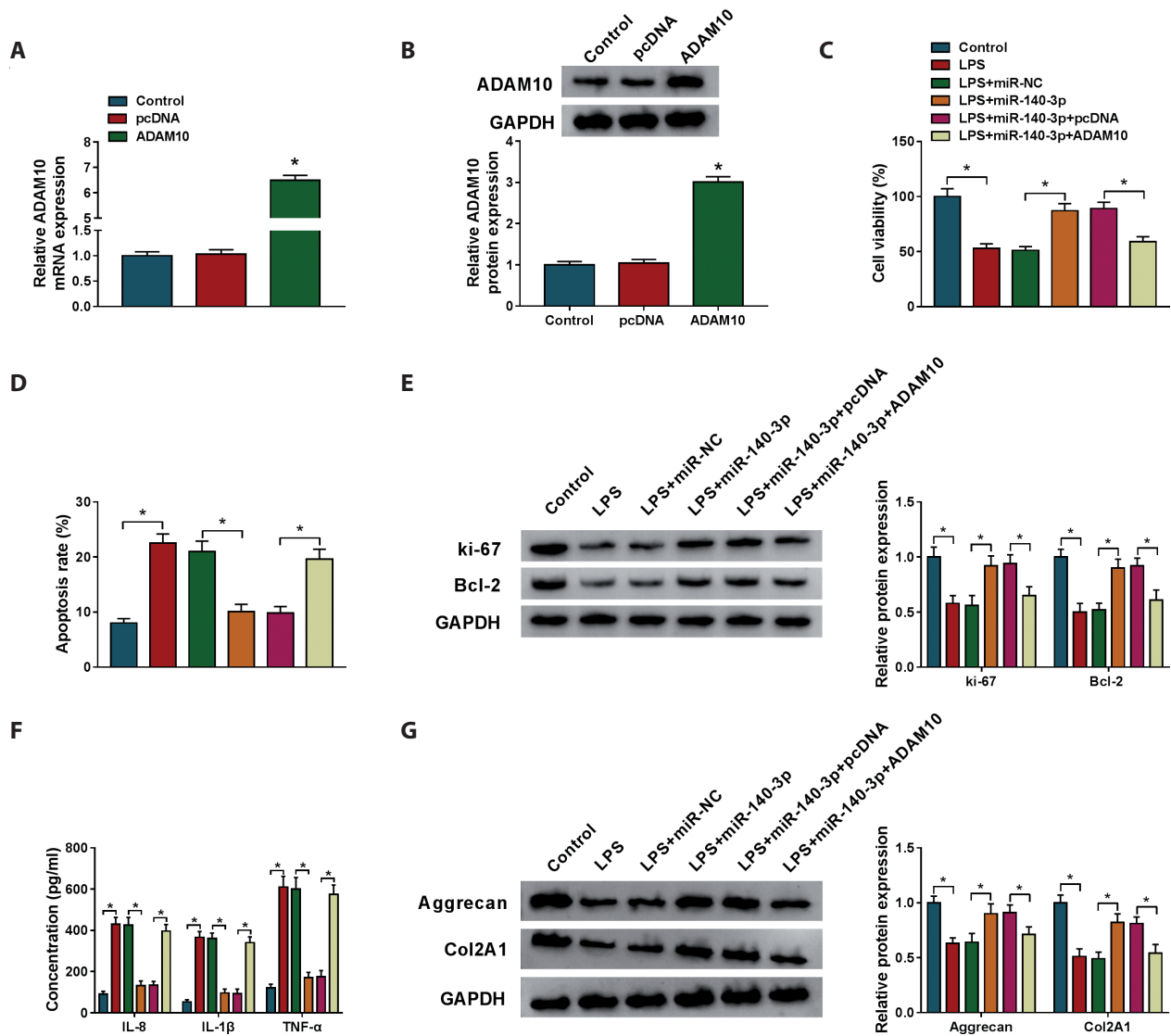


Figure 6. miR-140-3p overexpression alleviated LPS-evoked C-28/I2 cell injury and ECM loss by down-regulating ADAM10. **A, B.** ADAM10 mRNA and protein levels by qRT-PCR and Western blot assays in C-28/I2 cells transfected with pcDNA or ADAM10 overexpression plasmid. C-28/I2 cells were transfected with miR-NC mimic, miR-140-3p mimic, miR-140-3p mimic+pcDNA or miR-140-3p mimic+ADAM10 overexpression plasmid before 5 μg/ml of LPS treatment, followed by the detection of cell viability by CCK-8 assay (**C**), cell apoptosis by flow cytometry (**D**), ki-67 and Bcl-2 levels by Western blot (**E**), IL-8, IL-1β and TNF-α levels by ELISA assay (**F**), Aggrecan and Col2A1 levels by Western blot (**G**). * $p < 0.05$ by ANOVA followed by Tukey-Kramer *post hoc* test. For abbreviations, see Fig. 1 and 5.

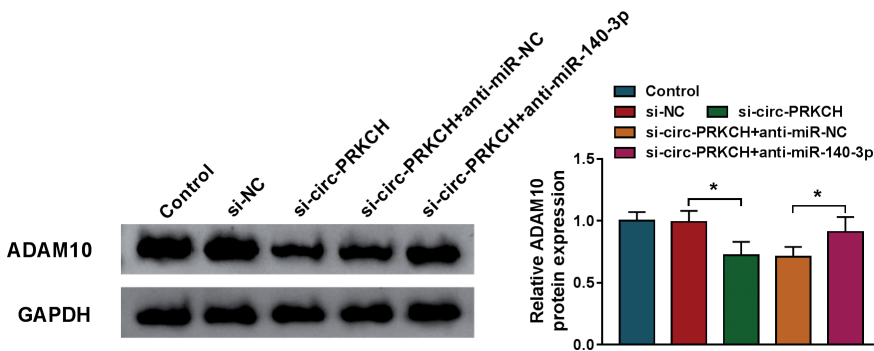


Figure 7. circ-PRKCH regulated ADAM10 expression through sponging miR-140-3p. C-28/I2 cells were transfected with or without si-NC, si-circ-PRKCH, si-circ-PRKCH+anti-miR-NC or si-circ-PRKCH+anti-miR-140-3p, followed by the assessment of ADAM10 expression by Western blot. * $p < 0.05$ by ANOVA followed by Tukey-Kramer *post hoc* test. For abbreviations, see Fig. 1 and 5.

sion through sponging miR-140-3p. Our work highlighted a novel target, the circ-PRKCH/miR-140-3p/ADAM10 axis, for OA management.

Conflict of interest. The authors declare that they have no financial conflicts of interest.

References

- Al-Modawi RN, Brinchmann JE, Karlsen TA (2019): Multi-pathway protective effects of microRNAs on human chondrocytes in an in vitro model of osteoarthritis. *Mol. Ther. Nucleic Acids* **17**, 776-790
<https://doi.org/10.1016/j.omtn.2019.07.011>
- Alabi RO, Farber G, Blobel CP (2018): Intriguing roles for endothelial ADAM10/notch signaling in the development of organ-specific vascular beds. *Physiol. Rev.* **98**, 2025-2061
<https://doi.org/10.1152/physrev.00029.2017>
- Charlier E, Deroyer C, Ciregia F, Malaise O, Neuville S, Plener Z, Malaise M, de Seny D (2019): Chondrocyte dedifferentiation and osteoarthritis (OA). *Biochem. Pharmacol.* **165**, 49-65
<https://doi.org/10.1016/j.bcp.2019.02.036>
- Chubinskaya S, Mikhail R, Deutsch A, Tindal MH (2001): ADAM-10 protein is present in human articular cartilage primarily in the membrane-bound form and is upregulated in osteoarthritis and in response to IL-1alpha in bovine nasal cartilage. *J. Histochem. Cytochem.* **49**, 1165-1176
<https://doi.org/10.1177/002215540104900910>
- Dallas DJ, Genever PG, Patton AJ, Millichip MI, McKie N, Skerry TM (1999): Localization of ADAM10 and Notch receptors in bone. *Bone* **25**, 9-15
[https://doi.org/10.1016/S8756-3282\(99\)00099-X](https://doi.org/10.1016/S8756-3282(99)00099-X)
- Dudekula DB, Panda AC, Grammatikakis I, De S, Abdelmohsen K, Gorospe M (2016): CircInteractome: A web tool for exploring circular RNAs and their interacting proteins and microRNAs. *RNA Biol.* **13**, 34-42
<https://doi.org/10.1080/15476286.2015.1128065>
- Ebell MH (2018): Osteoarthritis: rapid evidence review. *Am. Fam. Physician* **97**, 523-526
- Han B, Chao J, Yao H (2018): Circular RNA and its mechanisms in disease: From the bench to the clinic. *Pharmacol. Ther.* **187**, 31-44
<https://doi.org/10.1016/j.pharmthera.2018.01.010>
- Jiang W, Li T, Wang J (2019): miR-140-3p suppresses cell growth and induces apoptosis in colorectal cancer by targeting PD-L1. *Onco. Targets Ther.* **12**, 10275-10285
<https://doi.org/10.2147/OTT.S226465>
- Karlsen TA, Jakobsen RB, Mikkelsen TS, Brinchmann JE (2014): microRNA-140 targets RALA and regulates chondrogenic differentiation of human mesenchymal stem cells by translational enhancement of SOX9 and ACAN. *Stem Cells Dev.* **23**, 290-304
<https://doi.org/10.1089/scd.2013.0209>
- Kobayakawa T, Takahashi N, Sobue Y, Terabe K, Ishiguro N, Kojima T (2016): Mechanical stress loading induces CD44 cleavage in human chondrocytic HCS-2/8 cells. *Biochem. Biophys. Res. Commun.* **478**, 1230-1235
<https://doi.org/10.1016/j.bbrc.2016.08.099>
- Liu Q, Zhang X, Hu X, Dai L, Fu X, Zhang J, Ao Y (2016): Circular RNA related to the chondrocyte ECM regulates MMP13 expression by functioning as a MiR-136 'Sponge' in human cartilage degradation. *Sci. Rep.* **6**, 22572
<https://doi.org/10.1038/srep22572>
- Liu QP, Wu TH, Zheng H, Chen SJ, Chen YH, Chen L, Lin Z (2019): MiR-140-3p overexpression activates the Wnt signaling pathway to promote fracture healing. *Eur. Rev. Med. Pharmacol. Sci.* **23**, 6011-6017
- Malemud CJ (2018): MicroRNAs and osteoarthritis. *Cells* **7**, 92
<https://doi.org/10.3390/cells7080092>
- Martel-Pelletier J, Barr AJ, Cicuttini FM, Conaghan PG, Cooper C, Goldring MB, Goldring SR, Jones G, Teichtahl AJ, Pelletier JP (2016): Osteoarthritis. *Nat. Rev. Dis. Primers* **2**, 16072
<https://doi.org/10.1038/nrdp.2016.72>
- Mizuno S, Yoda M, Kimura T, Shimoda M, Akiyama H, Chiba K, Nakamura M, Horiuchi K (2020): ADAM10 is indispensable for longitudinal bone growth in mice. *Bone* **134**, 115273
<https://doi.org/10.1016/j.bone.2020.115273>
- Ntoumou E, Tzetzis M, Braoudaki M, Lambrou G, Poulou M, Malizos K, Stefanou N, Anastasopoulou L, Tsezou A (2017): Serum microRNA array analysis identifies miR-140-3p, miR-33b-3p and miR-671-3p as potential osteoarthritis biomarkers involved in metabolic processes. *Clin. Epigenetics* **9**, 127
<https://doi.org/10.1186/s13148-017-0428-1>
- Oo WM, Yu SP, Daniel MS, Hunter DJ (2018): Disease-modifying drugs in osteoarthritis: current understanding and future therapeutics. *Expert Opin. Emerg. Drugs* **23**, 331-347
<https://doi.org/10.1080/14728214.2018.1547706>
- Panda AC (2018): Circular RNAs act as miRNA sponges. *Adv. Exp. Med. Biol.* **1087**, 67-79
https://doi.org/10.1007/978-981-13-1426-1_6
- Patop IL, Wüst S, Kadener S (2019): Past, present, and future of circRNAs. *EMBO J.* **38**, e100836
<https://doi.org/10.15252/embj.2018100836>
- Qing Z, Ye J, Wu S (2019): Lipopolysaccharide-induced expression of astrocyte elevated gene-1 promotes degeneration and inflammation of chondrocytes via activation of nuclear factor-κB signaling. *Int. Immunopharmacol.* **71**, 84-92
<https://doi.org/10.1016/j.intimp.2019.03.006>
- Rasheed Z, Rasheed N, Al-Shaya O (2018): Epigallocatechin-3-O-gallate modulates global microRNA expression in interleukin-1β-stimulated human osteoarthritis chondrocytes: potential role of EGCG on negative co-regulation of microRNA-140-3p and ADAMTS5. *Eur. J. Nutr.* **57**, 917-928
<https://doi.org/10.1007/s00394-016-1375-x>
- Rivetti di Val Cervo P, Lena AM, Nicoloso M, Rossi S, Mancini M, Zhou H, Saintigny G, Dellambra E, Odorisio T, Mahé C, et al. (2012): p63-microRNA feedback in keratinocyte senescence. *Proc. Natl. Acad. Sci. USA* **109**, 1133-1138
<https://doi.org/10.1073/pnas.1112257109>
- Saito T, Tanaka S (2017): Molecular mechanisms underlying osteoarthritis development: Notch and NF-κB. *Arthritis. Res. Ther.* **19**, 94
<https://doi.org/10.1186/s13075-017-1296-y>
- Shen S, Wu Y, Chen J, Xie Z, Huang K, Wang G, Yang Y, Ni W, Chen Z, Shi P, et al. (2019): CircSERPINE2 protects against

- osteoarthritis by targeting miR-1271 and ETS-related gene. *Ann. Rheum. Dis.* **78**, 826-836
<https://doi.org/10.1136/annrheumdis-2018-214786>
- Toonen JA, Ronchetti A, Sidjanin DJ (2016): A disintegrin and metalloproteinase10 (ADAM10) regulates NOTCH signaling during early retinal development. *PLoS One* **11**, e0156184
<https://doi.org/10.1371/journal.pone.0156184>
- Verduci L, Strano S, Yarden Y, Blandino G (2019): The circRNA-microRNA code: emerging implications for cancer diagnosis and treatment. *Mol. Oncol.* **13**, 669-680
<https://doi.org/10.1002/1878-0261.12468>
- Wang J (2018): Casticin alleviates lipopolysaccharide-induced inflammatory responses and expression of mucus and extracellular matrix in human airway epithelial cells through Nrf2/Keap1 and NF- κ B pathways. *Phytother. Res.* **32**, 1346-1353
<https://doi.org/10.1002/ptr.6067>
- Wang L, Wu LF, Lu X, Mo XB, Tang ZX, Lei SF, Deng FY (2015): Integrated analyses of gene expression profiles digs out common markers for rheumatic diseases. *PLoS One* **10**, e0137522
<https://doi.org/10.1371/journal.pone.0137522>
- Wang Y, Wu C, Yang Y, Ren Z, Lammi MJ, Guo X (2019): Preliminary exploration of hsa_circ_0032131 levels in peripheral blood as a potential diagnostic biomarker of osteoarthritis. *Genet. Test Mol. Biomarkers* **23**, 717-721
<https://doi.org/10.1089/gtmb.2019.0036>
- Xiao K, Xia Z, Feng B, Bian Y, Fan Y, Li Z, Wu Z, Qiu G, Weng X (2019): Circular RNA expression profile of knee condyle in osteoarthritis by illumina HiSeq platform. *J. Cell Biochem.* **120**, 17500-17511
<https://doi.org/10.1002/jcb.29014>
- Xie Z, Shen P, Qu Y, Xu J, Zheng C, Gao Y, Wang B (2020): MiR-20a inhibits the progression of human arthritis fibroblast-like synoviocytes and inflammatory factor expression by targeting ADAM10. *Environ. Toxicol.* **35**, 867-878
<https://doi.org/10.1002/tox.22923>
- Yang CY, Chanalaris A, Troeberg L (2017): ADAMTS and ADAM metalloproteinases in osteoarthritis - looking beyond the 'usual suspects'. *Osteoarthritis Cartilage* **25**, 1000-1009
<https://doi.org/10.1016/j.joca.2017.02.791>
- Yin CM, Suen WC, Lin S, Wu XM, Li G, Pan XH (2017): Dysregulation of both miR-140-3p and miR-140-5p in synovial fluid correlate with osteoarthritis severity. *Bone Joint Res.* **6**, 612-618
<https://doi.org/10.1302/2046-3758.611.BJR-2017-0090.R1>
- Zhou Y, Wang B, Wang Y, Chen G, Lian Q, Wang H (2019a): miR-140-3p inhibits breast cancer proliferation and migration by directly regulating the expression of tripartite motif 28. *Oncol. Lett.* **17**, 3835-3841
<https://doi.org/10.3892/ol.2019.10038>
- Zhou Z, Du D, Chen A, Zhu L (2018): Circular RNA expression profile of articular chondrocytes in an IL-1 β -induced mouse model of osteoarthritis. *Gene* **644**, 20-26
<https://doi.org/10.1016/j.gene.2017.12.020>
- Zhou ZB, Huang GX, Fu Q, Han B, Lu JJ, Chen AM, Zhu L (2019b): circRNA.33186 contributes to the pathogenesis of osteoarthritis by sponging miR-127-5p. *Mol. Ther.* **27**, 531-541
<https://doi.org/10.1016/j.ymthe.2019.01.006>
- Zhu ZR, He Q, Wu WB, Chang GQ, Yao C, Zhao Y, Wang M, Wang SM (2018): MiR-140-3p is involved in In-stent restenosis by targeting C-Myb and Bcl-2 in peripheral artery disease. *J. Atheroscler. Thromb.* **25**, 1168-1181
<https://doi.org/10.5551/jat.44024>

Received: August 13, 2020

Final version accepted: January 1, 2021